

# Impact of Argon in Reforming of (CH<sub>4</sub> + CO<sub>2</sub>) in Surface Dielectric Barrier Discharge Reactor to Produce Syngas and Liquid Fuels

Abdelkader Rahmani<sup>1</sup> · Mehrdad Nikravech<sup>1</sup>

Received: 30 October 2017 / Accepted: 4 March 2018 / Published online: 10 March 2018  
© Springer Science+Business Media, LLC, part of Springer Nature 2018

**Abstract** The aim of this work is to study the role of argon during plasma reforming of methane and carbon dioxide in order to convert Biogas into liquid fuels. Mixtures of synthetic CH<sub>4</sub> and CO<sub>2</sub>, representing typical biogas compositions, were processed in a surface dielectric barrier discharge reactor in the presence of argon, which is considered to improve the discharge conditions. Our measurements showed that at constant feed flow rate and constant applied power, increasing the argon percentage from 0 to 66% in the feed, leads to increase the electron density up to 60% and the electron mean energy up to 50%. In these conditions, the absolute conversions of CH<sub>4</sub> and CO<sub>2</sub> are improved respectively from 19 to 43% and from 11 to 25%, the H<sub>2</sub>/CO ratio enhances up to 0.9. However, despite these improvements, the addition of argon beyond 33% decreases the carbon balance by deposition of black carbon and soot, decreases the selectivity of liquid products and finally lowers the energy efficiency of CH<sub>4</sub> + CO<sub>2</sub> mixture conversion. Meanwhile the selectivity of 10 liquid fuels principally alcohols, ketones and light organic acids, obtained in a yield of 3 wt%, depends also on the flow rate of argon in the feed mixture.

**Keywords** Biogas · Dry reforming · DBD · Liquid fuels · Argon

## Introduction

Biogas is a mixture of CH<sub>4</sub> and CO<sub>2</sub>, and is produced from the degradation of organic waste, is an important source of renewable energy. The energy value of biogas containing 60% of methane is estimated to be more than 7 kWh/Nm<sup>3</sup>. The annual potential of crude biogas in Europe by 2050 is estimated between 322 and 1050 Mtoe (Million Tonnes of Oil Equivalent) [1], while in 2013, only 13.4 Mtoe of primary energy was produced in Europe

---

✉ Mehrdad Nikravech  
nikravech@lspm.cnrs.fr

<sup>1</sup> LSPM-CNRS, Université Sorbonne Paris Cité, Université Paris 13, 99 Avenue Jean Baptiste Clément, 93430 Villetaneuse, France

from biogas [2]. As a result, biogas remains an underutilized source of renewable energy. The exploitation of this energy resource is a priority to replace hydrocarbons of fossil origin.

Currently, biogas is used as a fuel for internal combustion engines. In some production sites, biogas is injected, after 95% methane purification, into the natural gas grids. Development of a new route for the recovery of biogas into liquid fuels, such as acetone, methanol, ethanol and acetic acid, will achieve two objectives: reducing greenhouse gas emissions and producing high added-value products for the chemical industry. The reforming of methane in the presence of carbon dioxide, commonly called “Dry Reforming of Methane (DRM)”, is known for a long time [3], however presents some challenges including the requirement of working temperatures above 700 °C and the use of catalysts [4]. This reaction produces mainly hydrogen and carbon monoxide (syngas). This mixture can then be converted into liquid fuels by Fischer–Tropsch process.

The implementation of an efficient, rapid and cold-working device for conversion of biogas to liquid form would allow an increase in value of biogas produced in farms and in rural areas far from the gas transport networks. Plasma reactors meet all criteria necessary (i.e. energy characteristics) to perform biogas conversion. Different types of thermal plasma and cold plasma such as Dielectric Barrier Discharges (DBD), corona discharge, gliding-arc, plasma jet, spark and nanosecond pulsed discharge have been used to carry out DRM [5–8]. However, DBD remains the most used reactor for studying the DRM reaction because of its technical simplicity as well as the ease of scale up from laboratory reactors to large industrial plants [9]. In our case, we used a Surface Dielectric Barrier Discharge SDBD [10] which is different from the volume geometry i.e. cylindrical geometry generally reported in the literature [11–13]. In the cylindrical DBD configuration, the micro-discharges act as a bridge between the two electrodes separated by the gas and one (or two) dielectric barriers. Thus, the plasma volume is defined by the space between the two electrodes. On the other hand, in the SDBD, two electrodes are applied on both sides of a dielectric barrier sheet. Thus, there is no gap between the electrodes and the dielectric. In this case the plasma is formed on the dielectric barrier surface nearby the contact line of the electrodes and the dielectric. There are currently a single sided and double sided SDBD commonly in use. In single sided SDBD one of the electrodes covers entirely one side of the dielectric barrier while a second narrow metallic electrode is applied tightly on the other side. In double sided SDBD, two narrow electrodes are applied on both sides of the dielectric barrier as shown in Fig. 1.

An increase in the voltage results in an expansion of the discharge zone on the surface of the dielectric [9]. In this zone, the charges transfer takes place in micro-discharges, which appear on the surface of the dielectric barrier parallel to the flow direction of the gas stream. In this case, the activated species are rapidly quenched on the surface of the dielectric. This interrupts the chain reactions resulting in orientation of mechanisms to promote liquid products formation rather than synthesis gas. Furthermore, SDBD has been used in the past to study acetylene abatement and the production of ozone [14]. While no difference has been found between the performances of single-sided SDBD and double-sided SDBD geometry for acetylene abatement, double-sided geometry has shown better performances in ozone production. In addition, SDBD has shown to perform better than cylindrical geometry in acetylene abatement. The authors attributed this effect to the interaction of streamer with the surface of the dielectric over its entire length which not only allows to facilitate plasma initiation, but also to improve the use of atomic oxygen formed during the phase “On” of plasma. This shows that we cannot extrapolate the

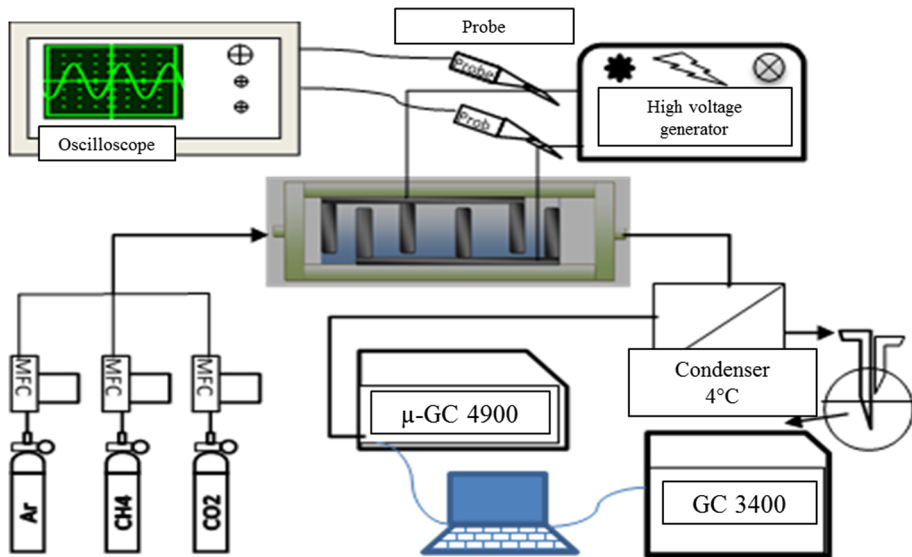


**Fig. 1** Experimental setup

performance of a reactor in a given application to other applications based on their geometries. Instead, the influence of geometry should be studied separately.

DRM by plasma processes has been studied for decades [15, 16]. Most of these works aim to produce mainly synthesis gas and only few studies deal with formation of liquid products [17]. The influence of Ar on the distribution of liquid products of the DRM in a SDBD has not been studied to our knowledge. Ramakers et al. [18] studied the role of argon and helium on the CO<sub>2</sub> conversion in a cylindrical DBD. They demonstrated that CO<sub>2</sub> conversion increases using Ar and He, and that the effect of Ar is greater than that of He. On the other hand, the energy efficiency decreases by adding Ar because a considerable part of the energy is consumed to ionize and excite Ar and He atoms [18]. Jo et al. [19] carried out a comparative study of the influence of noble gases in particular: He, Ne, Ar, Kr, and Xe on the conversion of CH<sub>4</sub> in a DBD. The total flow rate of the reactant stream containing 90% of noble gas was set at 336 mL/min, and the mean power was varied between 4 and 20 W. The products of the transformation were mainly alkanes such as C<sub>2</sub>H<sub>6</sub> and C<sub>3</sub>H<sub>8</sub>. They were produced independently of the noble gas. The addition of Kr allowed them to have the best conversion under the same conditions.

Pinhao et al. [20] and Goujard et al. [21] studied the influence of He on DRM in a DBD. The major products of the reaction were: H<sub>2</sub>, CO, C<sub>2</sub>H<sub>6</sub> and C<sub>3</sub>H<sub>8</sub> and traces of condensable liquid fuels. They demonstrated that He reduces breakdown voltage and improves the conversions of CH<sub>4</sub> and CO<sub>2</sub>. Ozkan et al. [22] designed a multi-electrodes cylindrical reactor to treat high flow rates of biogas. The total flow rate of the reactants was set at 1920 mL/min with 93.75% of plasma gas feed in argon or helium. The authors reported that the conversion and energy efficiency were higher in the presence of plasma gas. They also demonstrated that in the presence of argon, a filamentary aspect dominated the plasma and favored the conversion of CO<sub>2</sub> whereas in the presence of helium, the filamentary plasma was transformed into glow plasma and the conversion of CH<sub>4</sub> was favored. This effect has been attributed to the influence of plasma gas on electrons energy distribution's

function. Zhang et al. [23] studied the influence of several parameters on the DRM in a cylindrical DBD such as the power, the flow rate, the ratio  $\text{CH}_4/\text{CO}_2$ , the percentage of argon as well as the introduction of solid particles in the plasma acting as a catalyst. They reported that argon stabilizes the plasma and improves the conversion of biogas. However, the addition of argon had no influence on the  $\text{H}_2/\text{CO}$  ratio. Janeco et al. [24] developed a self-consistent numerical model to describe the influence of helium dilution on electronic kinetics in a gas mixture of  $\text{He}/\text{CH}_4/\text{CO}_2/\text{CO}/\text{H}_2$ . These authors considered the filamentary appearance of the DBD discharge at room temperature. Although not all chemical species that may be present in plasma have been considered, model's results demonstrate that helium decreases the number of electrons with low energy and increases the number of energetic electrons. The authors attributed this effect to the threshold energy of inelastic collisions in a mixture of molecular gases globally smaller compared to a mixture containing helium.

## Experimental Setup and Methods

The SDBD reactor used in this experiment consists of a dielectric plate made of quartz glass with a length of 150 mm, a width of 60 mm and a thickness of 3 mm. Two “E” shaped aluminum electrodes with a thickness of 3 mm are installed on both sides of the dielectric plate as shown in Fig. 1. Two quartz glass plates cover the top and bottom of this assembly, and two ceramic parts ensure electrical insulation and sealing of the reactor.

The power supply of this SDBD is provided by a high-voltage AC current generator (18 kV peak to peak), and a frequency of 33 kHz. Three “Bronkhorst” mass flowmeters were used to monitor the flow of each reactant. The material balance on liquid and gaseous products is established on the basis of chromatographic methods. We used a gas chromatograph (VARIAN 3400) for the analysis of liquid products, and a gas chromatograph (VARIAN CP4900) for the analysis of gaseous products.

The energy balance is established by measuring electrical charges that pass through the reactor. This measurement is carried out by the LISSAJOUS (Manley) method using two resistive probes connected to an oscilloscope (Lecroy) with a 350 MHz acquisition frequency. Data acquisition and calculations are performed via a Labview program on a computer linked to the oscilloscope. A condenser is installed at the outlet of the reactor to recover the liquid products at 4 °C. The condenser contains 5 mL of pure water which acts as an absorbent. More than 90% of the condensate fuels are trapped. The saturated vapor pressure of these products does not allow a completely condensation at 4 °C. Gaseous products are analyzed with a calibrated Varian microGC 4900. The identification of the liquid products was performed by a GC-MS Shimadzu. The quantitative analysis of the liquids was carried out with a gas chromatograph Varian GC 3400 equipped with FID detector and a capillary column Agilent DB 624 (60 m, 0.32 mm, 1.8  $\mu\text{m}$ ) suitable to separate polar hydrocarbons.

Preliminary results concerning the effect of plasma-catalysis have been published in [10]. The reactivity in plasma is directly related to electron density and electron temperature. However, these parameters depend mainly on the composition of gas mixture, applied power and configuration of the reactor. In this work, we study the role of argon on the discharge and its consequences on the efficiency of the  $\text{CH}_4\text{--CO}_2$  transformation, as well as on the yield and the selectivity of the products in a SDBD. The absolute and the

effective conversion, selectivity of gaseous products and carbon balance were defined as in the literature [23, 25, 26].

$$\text{CH}_4 \text{ abs. conversion (\%)} = \frac{\text{moles of CH}_4 \text{ converted}}{\text{moles of CH}_4 \text{ introduced}} \times 100 \quad (1)$$

$$\text{CO}_2 \text{ abs. conversion (\%)} = \frac{\text{moles of CO}_2 \text{ converted}}{\text{moles of CO}_2 \text{ introduced}} \times 100 \quad (2)$$

$$\text{CH}_4 \text{ effec. conversion (\%)} = \text{CH}_4 \text{ abs. conversion (\%)} \times \frac{\text{moles of CH}_4 \text{ introduced}}{\text{total moles introduced}} \times 100 \quad (3)$$

$$\text{CO}_2 \text{ effec. conversion (\%)} = \text{CO}_2 \text{ abs. conversion (\%)} \times \frac{\text{moles of CO}_2 \text{ introduced}}{\text{total moles introduced}} \times 100 \quad (4)$$

$$\text{CO selectivity (\%)} = \frac{\text{moles of CO produced}}{(\text{moles of CH}_4 \text{ converted}) + (\text{moles of CO}_2 \text{ converted})} \times 100 \quad (5)$$

$$\text{H}_2 \text{ selectivity (\%)} = \frac{\text{moles of H}_2 \text{ produced}}{2 \times \text{moles of CH}_4 \text{ converted}} \times 100 \quad (6)$$

$$\text{C}_x\text{H}_y \text{ selectivity (\%)} = \frac{x \times \text{moles of C}_x\text{H}_y \text{ produced}}{(\text{moles of CH}_4 \text{ converted}) + (\text{moles of CO}_2 \text{ converted})} \times 100 \quad (7)$$

$$\text{B}_{\text{carbone}} (\%) = \frac{[\text{CH}_4]_{\text{out}} + [\text{CO}_2]_{\text{out}} + [\text{CO}]_{\text{out}} + \sum x \times [\text{C}_x\text{H}_y\text{O}_z]}{[\text{CH}_4]_{\text{in}} + [\text{CO}_2]_{\text{in}}} \times 100 \quad (8)$$

## Results and Discussions

### Influence of Ar on the Behavior of the Discharge and the Breakdown Voltage of the CH<sub>4</sub>–CO<sub>2</sub> Mixture

The Ar percentage in the CH<sub>4</sub>–CO<sub>2</sub> mixture was varied from 0 to 66%, the CH<sub>4</sub>/CO<sub>2</sub> molar ratio was set at 1 while the reactants total flow rate was fixed at 120 mL/min and the applied power was fixed up to 74 W ± 2. The first observation of dilution by Ar was a change in plasma behavior (Fig. 2). Indeed, the number of micro-discharges increases when Ar percentage is increased.

Figure 2 shows also a greater homogeneity of the plasma when Ar percentage in the CH<sub>4</sub>–CO<sub>2</sub> mixture increases from 0 to 66% for a similar applied power. We also found that the breakdown voltage, determined by the Lissajous curve, decreases as a function of Ar percentage in the reactive stream as is shown in Fig. 3. The breakdown voltage decreases

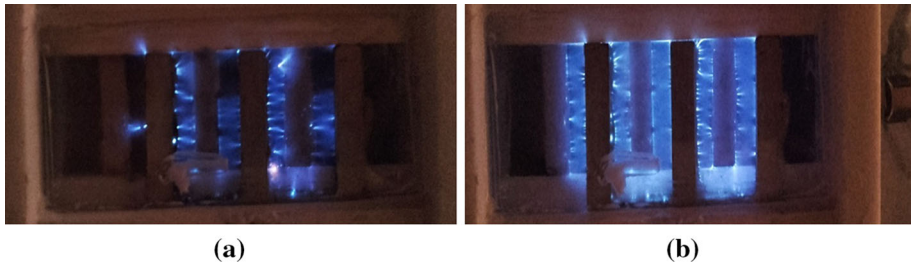


**Fig. 2** Pictures of the SDBD with  $\text{CH}_4\text{-CO}_2$  mixtures: SDBD without argon (a) and containing 66% Ar (b). a 73 W, 0%Ar. b 74 W, 66%Ar

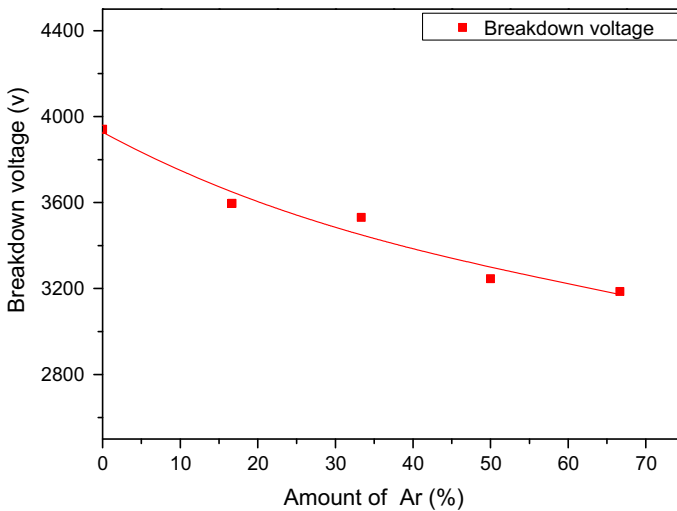


**Fig. 3** Evolution of breakdown voltage as a function of the amount of Ar at applied power of 74 W

from 3.95 to 3.30 kV when Ar percentage increases to 66%. This result is in agreement with those found by [18–21].

Ramakers et al. [18] explained this behavior by a Townsend ionization coefficient for Ar higher than that of  $\text{CO}_2$ , and a greater average free path for a mixture of  $\text{CO}_2\text{-Ar}$ . Indeed, the Townsend coefficient describes the production of electrons per unit length. A mixture with a high ionization coefficient does not require a high voltage to initiate the plasma. Sebastian and Wadehra [27] developed a model based on Boltzmann equation to calculate various parameters of a  $\text{CH}_4\text{-Ar}$  plasma, including the Townsend ionization coefficient. They found that the latter coefficient increases as a function of Ar percentage.

Another consequence of dilution with argon is the modification of the mean free path of electrons. Indeed, the probability of inelastic collisions for Ar is low compared to that of  $\text{CO}_2$  or  $\text{CH}_4$ . For Ar, electron excitation and ionization are the only possible inelastic collisions and are characterized by a relatively high activation energy threshold (11.55 and 15.76 eV, respectively). This is not the case for  $\text{CH}_4$  and  $\text{CO}_2$ , where there are different possible levels of vibrational, electronic, ionization and dissociation excitation. Thus, the presence of Ar, decreases the inelastic collisions frequency resulting in higher electron's energy. Moreover, the probability of attachment of electrons with  $\text{Ar}^+$  is lower than that

with  $\text{CO}_2^+$  due to the absence of dissociative attachment reactions in the case of Ar [18]. Consequently, in presence of Ar, the mean free path increases so electrons accelerate in the electric field and acquire a greater energy between two collisions. Thus, a low breakdown voltage is sufficient to initiate the plasma.

### Influence of Ar on Electron Density

In order to study the influence of Ar on the density and the electron energy, the Eq. (9) of current density was used:

$$n_e = \frac{J}{E\mu_e e} \tag{9}$$

where  $n_e$ : is the electron density. J: Current density defined as the ratio between maximum current, measured by Rogowski’s coil, and surface area of one micro-discharge ( $1.05 \times 10^{-6} \text{ m}^2$ ) [18]. E: Electric field (Td) determined by the breakdown voltage, the distance between the electrodes and gas density.  $\mu_e$ : Electron mobility calculated with Bolsig+, and e is the electron charge.

Several authors use this equation to estimate the density and energy of electrons [18, 28, 29]. The Maxwellian distribution of electrons is assumed to facilitate the resolution of Boltzmann equation by the Bolsig+ calculation code [30]. The secondary mechanisms are therefore neglected, in particular super-elastic or de-excitation collisions, inelastic collisions between excited states and electron-ion recombination. The reactions of moment transfer, excitation and ionization are taken into consideration.

Calculations results (Fig. 4) show that the density and electron temperature increase as a function of Ar percentage. The mean energy of electrons increases from 1 eV to almost 2 eV, when Ar percentage is increased from 0 to 66%. The electron density increases from  $10^{19}$  to  $1.6 \times 10^{19} \text{ m}^{-3}$ , an increase of 60%, as shown in Fig. 4. The two hypothesis to explain the decrease in breakdown voltage are also valid for this increase in electron’s

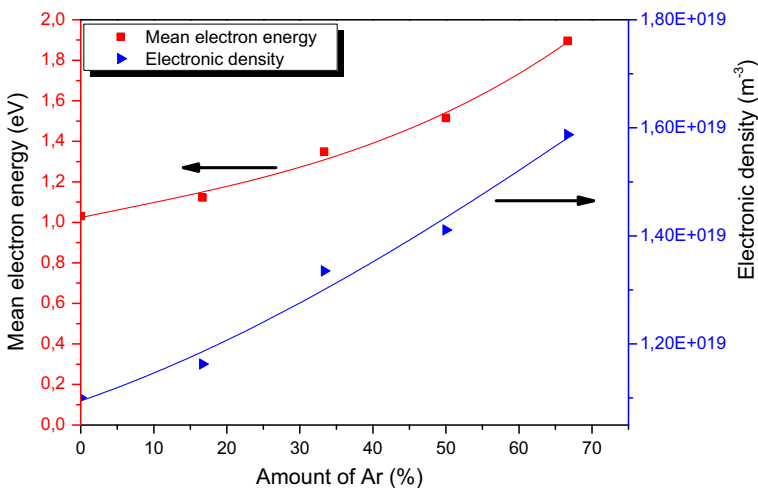


**Fig. 4** Evolution of mean energy of electrons and electron density as a function of the amount of Ar at applied power of 74 W

density and temperature. However, we should be prudent concerning the absolute value of electrons density since the surface micro-discharge values are roughly estimated [18].

### Influence of Ar Dilution on Conversion and Reactivity

The  $\text{CH}_4$  and  $\text{CO}_2$  conversions increase from 19 to 43%, and from 12 to 25%, respectively, when Ar percentage increases to 66% at applied power of  $74 \text{ W} \pm 2$  (Fig. 5). The same trend has been observed at applied power of  $51 \text{ W} \pm 2$ . The difference between reactants conversions seems to be related to the bond energy in each molecule. Indeed, the bond energy C–H in the  $\text{CH}_4$  molecule is equal to 4.3 eV/molecule, whereas the double bond energy C=O of  $\text{CO}_2$  is equal to 8.3 eV/molecule. The difference in the electron impact cross section mainly comes from the bond energy, but also from the collision probability explains also the more important dissociation of  $\text{CH}_4$  compared to  $\text{CO}_2$ . We observe that the conversion at 51 W is lower than that at 74 W due to the fact that the electron energy and electron density are lower at low specific energy [25].

Snoeckx et al. [31] have developed a 0D model to describe DRM in a cylindrical DBD at ambient temperature and atmospheric pressure. They found a significant difference between  $\text{CH}_4$  and  $\text{CO}_2$  conversions, and they justify it by a difference in binding energy in the two molecules. The authors concluded that  $\text{CO}_2$  transformation is mainly due to collisions with free radicals during “Off” phases of a microdischarge. On the other hand,  $\text{CH}_4$  transformation is due to collisions with electrons during “On” phases of a microdischarge as well as to collisions with free radicals during the “Off” phases of this microdischarge.

The addition of Ar to reactive flux leads to an increase in density and electron temperature as explained in “[Influence of Ar on Electron Density](#)” section, which leads to an increase of the number and the efficiency of electron collisions with the reactants, and thus increasing the conversions. In their work on the influence of argon in  $\text{CO}_2$  conversion, Ramakers et al. [18] reported that transfer of charges between  $\text{Ar}^+$ ,  $\text{Ar}^{++}$  and  $\text{CO}_2$  followed by an electron-ion dissociative attachment reaction of  $\text{CO}_2^+$  can be a very important mechanism for  $\text{CO}_2$  dissociation. We believe that the same mechanism can be present in

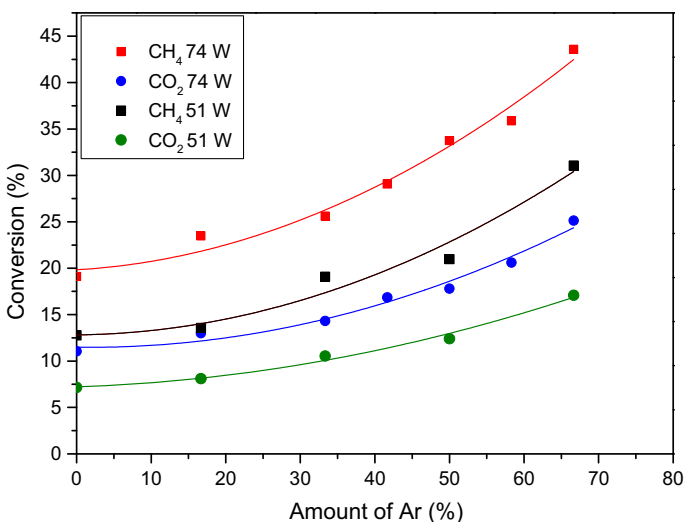


**Fig. 5** Evolution of  $\text{CH}_4$  and  $\text{CO}_2$  conversion as a function of the amount of Ar for 51 W and 74 W



DRM and especially favored in the presence of argon as shown by the set of reactions cited in Table 1.

Another explanation is to consider the Penning ionization effect, which corresponds to a transfer of energy from excited Ar\* atoms to CH<sub>4</sub> or CO<sub>2</sub>, which could dissociate these two molecules or at least ionize them. Attachment reactions thereafter could dissociate these ionized molecules. The same explanation was given by Goujard et al. [21]. On the other hand, the calculations made by Janeco and his collaborators have shown that helium absorbs less than 5% of the energy injected into the plasma, because of the large cross-section of the molecular gases and also the high threshold of inelastic collisions of helium. As a result, the authors affirmed that the Penning effect cannot compete with direct electronic collisions ionization [24].

In our case, the initial quantities of CH<sub>4</sub> and CO<sub>2</sub> decrease in favor of the quantity of argon in order to have a fixed total flow rate (120 mL/min). Therefore the residence time and the specific energy remain constant to allow the study of the role of argon. The same reasoning is adopted in all articles that deal with the influence of argon or helium on CO<sub>2</sub> splitting or CH<sub>4</sub> reforming by atmospheric plasma [18–21]. Thus, absolute conversion is a parameter not sufficient to fully describe the efficiency of the process. Indeed, to take into consideration the dilution effect of argon, we need to calculate the effective conversion. This can be seen in Fig. 6 where effective conversion for both reactants decreases as a function of Ar percentage. Methane effective conversion decreases from 9.5 to 7.3% by increasing Ar percentage from 0 to 66% at applied power of 74 W ± 2 while dioxide carbon effective conversion decreases from 5.5 to 4.2%. The same trend has been observed at applied power of 51 W ± 2.

### Influence of Ar Dilution on Energy Efficiency

In literature, there exist several definitions for energy efficiency. The first one is based on the enthalpy of transformation of methane and carbon dioxide into H<sub>2</sub> and CO. The sum of effective conversion for methane and carbon dioxide is used to calculate this energy efficiency as following:

$$\eta(\%) = \frac{\text{Total effect. conversion} \times \Delta H_{298}^{\circ} \left(\frac{\text{eV}}{\text{molecule}}\right)}{\text{SEI} \left(\frac{\text{eV}}{\text{molecule}}\right)} \times 100 \tag{10}$$

where SEI is the specific energy input, defined as the ratio between the power injected into the plasma and the total flow rate of the reactants. ΔH<sub>298</sub><sup>o</sup> is the enthalpy of the reaction of

**Table 1** Elementary reactions of CH<sub>4</sub> and CO<sub>2</sub> transformation and their rate coefficients [32, 33]

Reaction		Coefficient rate (cm <sup>3</sup> s <sup>-1</sup> )
e + Ar → Ar <sup>+</sup> + 2e	(1)	2.40 × 10 <sup>-16</sup>
Ar <sup>+</sup> + CH <sub>4</sub> → Ar + CH <sub>4</sub> <sup>+</sup>	(2)	2.94 × 10 <sup>-11</sup>
Ar <sup>+</sup> + CH <sub>4</sub> → Ar + CH <sub>3</sub> <sup>+</sup> + H	(3)	8.33 × 10 <sup>-10</sup>
Ar <sup>+</sup> + CO <sub>2</sub> → Ar + CO <sub>2</sub> <sup>+</sup>	(4)	5.00 × 10 <sup>-10</sup>
e + CH <sub>4</sub> <sup>+</sup> → CH <sub>3</sub> + H	(5)	1.18 × 10 <sup>-08</sup>
e + CH <sub>4</sub> <sup>+</sup> → CH <sub>2</sub> + 2H	(6)	2.42 × 10 <sup>-08</sup>
e + CH <sub>4</sub> <sup>+</sup> → CH + H <sub>2</sub> + H	(7)	1.41 × 10 <sup>-08</sup>
e + CO <sub>2</sub> <sup>+</sup> → CO + O	(8)	2.71 × 10 <sup>-07</sup>

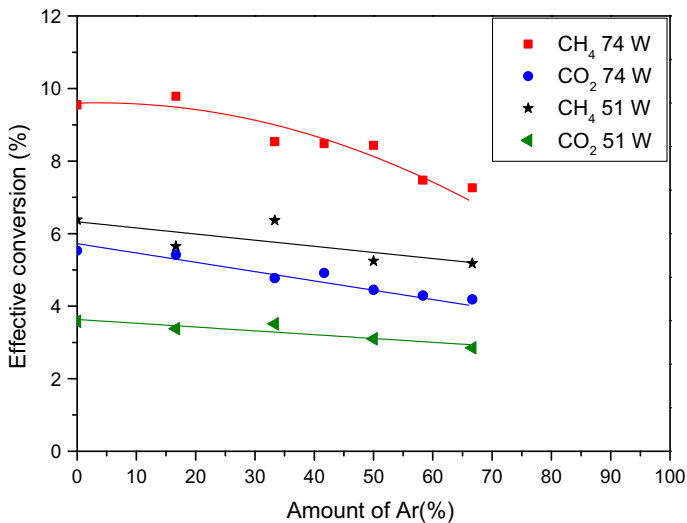


**Fig. 6** Evolution of the effective conversion as a function of the amount of Ar for 51 W and 74 W

transformation of biogas into syngas, estimated at 2.56 eV/molecule. This formula doesn't take into account the formation of higher hydrocarbons.

Although in the literature [8], it is reported that increasing the specific energy results in decreasing the energy efficiency of DRM, we do not observe this effect as there is not a big difference between both specific energies imposed in our study. On the other hand, the energy efficiency decreases from 4.2 to 3.0% at applied power of  $74 \text{ W} \pm 2$  as shown in Fig. 7a. The same trend has been observed at applied power of  $51 \text{ W} \pm 2$  (Fig. 7b). With a high Ar content, the excitation reactions of Ar consume a part of energy injected into the plasma. The de-excitation reactions against the walls of the reactor and the natural relaxation of these excited species prevent them to participate in biogas conversion. The decrease of effective conversion of both reactants, as shown in “[Influence of Ar Dilution on Conversion and Reactivity](#)” section, also explains this decrease in energy efficiency. The energy efficiency depends on several parameters including, for example: the specific energy, the frequency as well as the type of the power supply and the composition of the feed gas. It is then quite difficult to compare the efficiency of two different geometries. Under conditions similar to the conditions imposed in this study, Snoeckx et al. [26] reported that the cylindrical DBD efficiency was between 2.8 and 6%. Thus, SDBD shows the same energy efficiency of cylindrical DBD for the DRM.

However, the formula (10) assumes that biogas is transformed only into syngas and that the conversions of CH<sub>4</sub> and CO<sub>2</sub> are similar. This makes it easier to calculate the stoichiometric subscripts of the reaction and consequently the estimation of reaction enthalpy which is equal to 2.56 eV/molecule. However, the DRM in a plasma reactor is more complicated than that. Indeed, CH<sub>4</sub> conversion is greater than that of CO<sub>2</sub>, and other gaseous and liquid products are formed in addition to syngas.

This leads us to define a second energy efficiency which takes into account the Lower Heating Value (LHV) of the chemicals products. In this case, energy efficiency is defined as the ratio between sum LHV of products (liquid and gaseous) divided by the input energy that is the summation of the electrical energy of plasma and the LHV of converted methane. The energy efficiency of the process is calculated using the following formula:

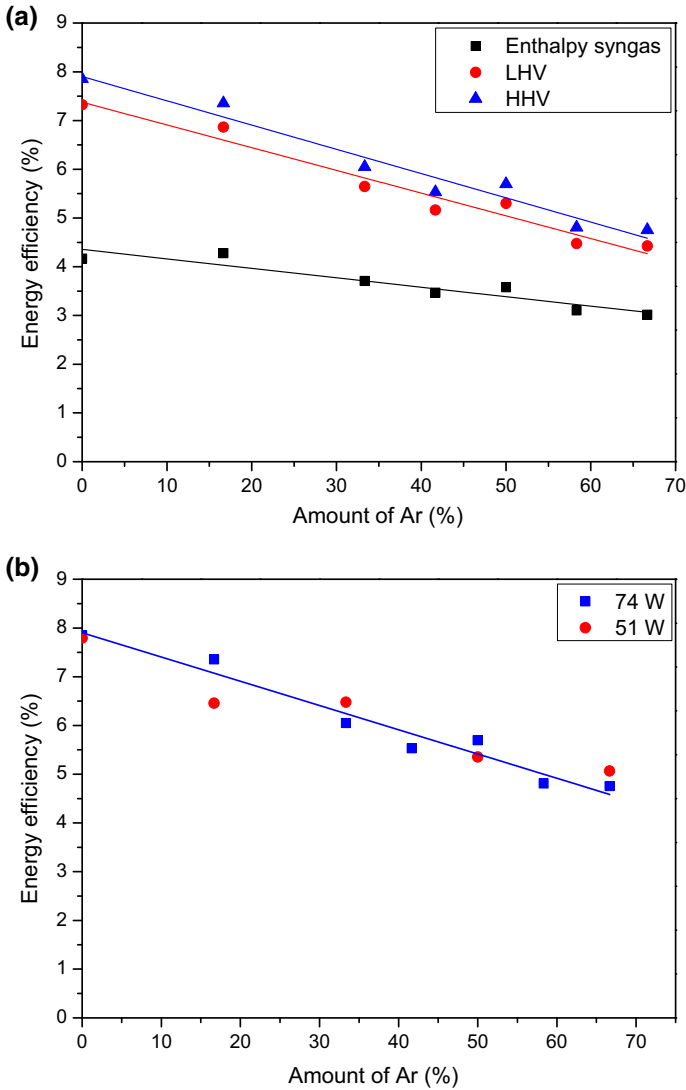


**Fig. 7** **a** Comparative of energy efficiency as a function of the amount of Ar for 74 W, estimated by using Enthalpy syngas Eq. (11), LHV using Eq. (12) and HHV using Eq. (13). **b** Evolution of energy efficiency HHV as a function of the amount of Ar for 74 and 51 W

$$\eta (\%) = \frac{[\sum [i] \times LHV (i)]}{Applied\ power + [CH_4] \times LHV(CH_4) \times CH_4\ abs.\ conversion (\% )} \quad (11)$$

where [i] is the produced amount of product (i) or its amount in feed gas expressed in Nm<sup>3</sup>/s for gaseous products and in g/s for liquid products, LHV(i) is the lower heating value of the product (i) expressed in J/ Nm<sup>3</sup> for gaseous products and in kJ/kg for liquid products.

The third energy efficiency is defined by taking into consideration the Higher Heating Values (HHV) of different fuels as following:

$$\eta (\%) = \frac{[\sum[i] \times \text{HHV}(i)]}{\text{Applied power} + [\text{CH}_4] \times \text{HHV}(\text{CH}_4) \times \text{CH}_4 \text{ abs. conversion} (\%)} \quad (12)$$

The results using these three definitions are plotted in the same graph for comparison (Fig. 7a). We can see that at a low percentage in Ar, taking into consideration the heating values of higher hydrocarbons, i.e.  $\text{C}_2\text{H}_4$ ,  $\text{C}_2\text{H}_6$  and liquid products doubles the energy efficiency of the DRM process. On the other hand, with a high percentage in Ar, the difference between the results of these last three definitions becomes relatively small. This is due to a decrease in the selectivity of the process towards the formation of high added value hydrocarbons, i.e.  $\text{C}_2\text{H}_6$  and  $\text{C}_2\text{H}_4$  as well as liquid oxygenates, at a high percentage of Ar. The decrease in the selectivity of these latter products will be discussed in the next two paragraphs. Calculating the energy efficiency as a function of the HHV improves slightly the value of energy efficiency with respect to the calculation results based on the LHV. On the other hand, adding liquid products has no noticeable effects on the value of energy efficiency because of the small quantity of liquid products but also the low values of their heating values.

### Influence of Dilution by Ar on the Selectivity of Gaseous Products

The analysis of gaseous products of the reaction reveals that  $\text{H}_2$ , CO,  $\text{C}_2\text{H}_4$  and  $\text{C}_2\text{H}_6$  are the main products of DRM under our experimental conditions. The selectivity to  $\text{H}_2$  and CO formation increases as a function of Ar percentage while the selectivity towards  $\text{C}_2\text{H}_4$  and  $\text{C}_2\text{H}_6$  formation decreases, as shown in Fig. 8. For example, the  $\text{C}_2\text{H}_6$  selectivity decreases from 18 to 11% when Ar percentage increases from 0 to 66% and the selectivity of  $\text{C}_2\text{H}_4$  decreases from 1 to 0.6%. The first hypothesis to explain this trend is the dilution of the reactive mixture by Ar. Indeed, the high Ar content reduces the molar fraction of all free radicals including  $\text{CH}_3$  which reduces the recombination's probability of these later free radicals. This decreases the production of ethane even if it is a three-body reaction (11). This hypothesis could be extrapolated to explain the decrease in

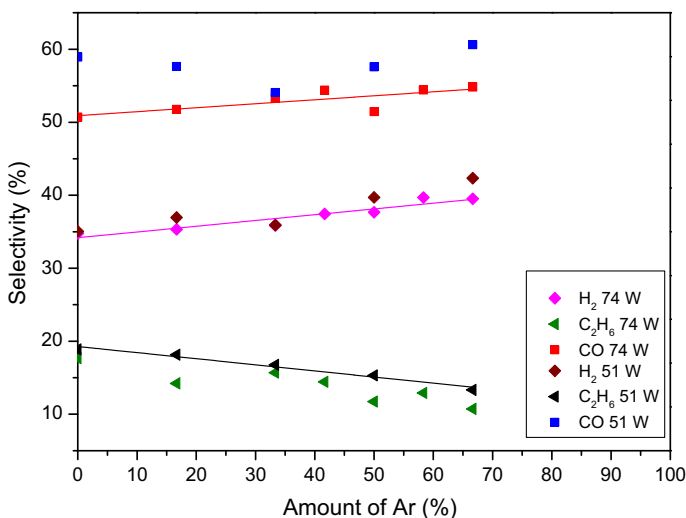


**Fig. 8** Evolution of selectivity as a function of the amount of Ar for 51 and 74 W

ethylene selectivity. A second hypothesis consists of considering an advanced degradation of CH<sub>4</sub> and CO<sub>2</sub> favored by a higher density and electron temperature in high Ar percentage, as shown in “Influence of Ar on Electron Density” section.

Indeed, H<sub>2</sub> and C are the ultimate products of the advanced degradation of CH<sub>4</sub>, as O and CO are for CO<sub>2</sub>, as shown by reactions (9) and (10):

$\text{CH}_4 + e \rightarrow \text{C} + 2\text{H}_2 + e$	(9)	[32]
$\text{CO}_2 + e \rightarrow \text{CO} + \text{O} + e$	(10)	[32]
$\text{CH}_3 + \text{CH}_3 + \text{M} \rightarrow \text{C}_2\text{H}_6 + \text{M}$	(11)	[34]
$\text{CH}_3 + \text{CH}_2 \rightarrow \text{C}_2\text{H}_4 + \text{H}$	(12)	[34]

The evolution of H<sub>2</sub>/CO ratio and that of carbon balance are depicted in Fig. 9. One can remark that the trends of these curves change when Ar percentage reaches 33% in the mixture. The carbon balance is defined as the ratio of total quantity of carbon leaving the reactor to the total amount of carbon at the reactor inlet. Thus, this parameter allows calculating the amount of carbon deposited on the walls of the reactor in the form of soot and black carbon plus the amount of species that have not been detected in the gas phase and liquid phase. As it is shown in Fig. 9, the carbon balance is relatively stable around 95% when Ar percentage increases from 0 to 33%, then decreases strongly to 90% when Ar percentage reaches 66%, at applied power of 74 W, indicating that increasing Ar percentage results in increasing soot formation into the SDBD instead of hydrocarbons.

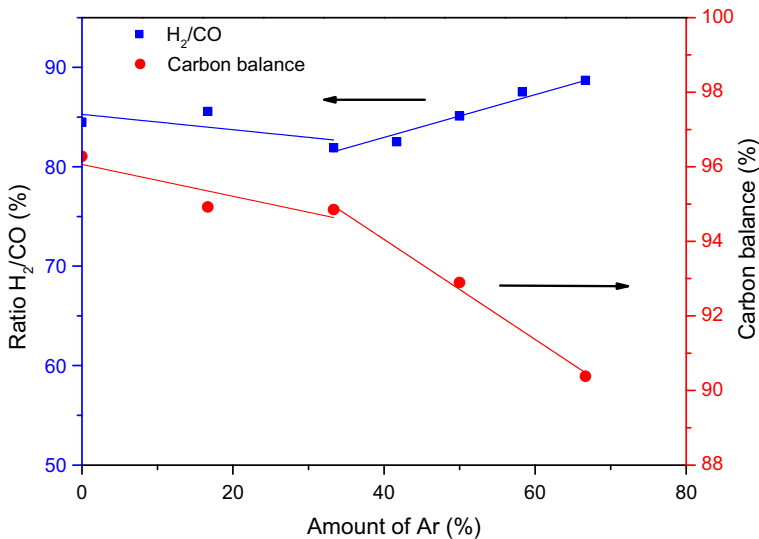


**Fig. 9** Evolution of H<sub>2</sub>/CO ratio and the carbon balance as a function of the amount of Ar at applied power of 74 W

## Influence of Ar Dilution on Liquid Products

The conversion of biogas by plasma SDBD leads to the formation of gaseous products and liquid products. The liquids were separated by condensation at 4 °C for 1 h. The selectivity of the produced liquid is defined as follows:

$$\text{Liquid selectivity (wt\%)} = \frac{\text{Liquid produced total mass}}{(\text{mass of CH}_4 \text{ converted}) + (\text{mass of CO}_2 \text{ converted})} \times 100 \quad (13)$$

The liquid selectivity, shown in Fig. 10, increases slightly from 15 to 16% when Ar percentage increases from 0 to 33% then decreases drastically for higher Ar percentage. These results underline that beyond 33% of argon in the mixture, the selectivity of liquids decreases and at the same time we visually observed that the quantity of carbon and of soot deposited on the reactor's walls increases. The changes in trends of liquid production observed in our conditions, 74 W and feed composition of (Ar–CH<sub>4</sub>–CO<sub>2</sub>) = (40–40–40 mL/min), correspond to the mean electrons energy and electron density respectively 1.3 eV and  $1.35 \times 10^{19} \text{ m}^{-3}$ . Liquid fuels represent between 10 and 30% of the total mass of liquid products, the rest consists of unidentified liquid products and especially water produced by Water Gas Shift Reaction. This liquid fuels represent from 2 to 4% of the total mass of CH<sub>4</sub> and CO<sub>2</sub> transformed.

Liquid hydrocarbon selectivity is defined as the mass ratio of the liquid compound in question and the total mass of liquid fuels. The distribution of liquid products, as a function of Ar percentage represented in Fig. 11, shows that the main products are: tertibutylic (2.5–3.8% w), acetaldehyde (11.4–13.9% w), acetone (3.4–4.8% w), 2-butanol (7.3–10.6% w), methanol (19.3–23.8% w), isopropanol (11.4–13.9% w), ethanol (15.1–18.1% w), propanol (3.0–5.8% w), butanol (5.8–12.4% w), and acetic acid (6.4–10.4% w).

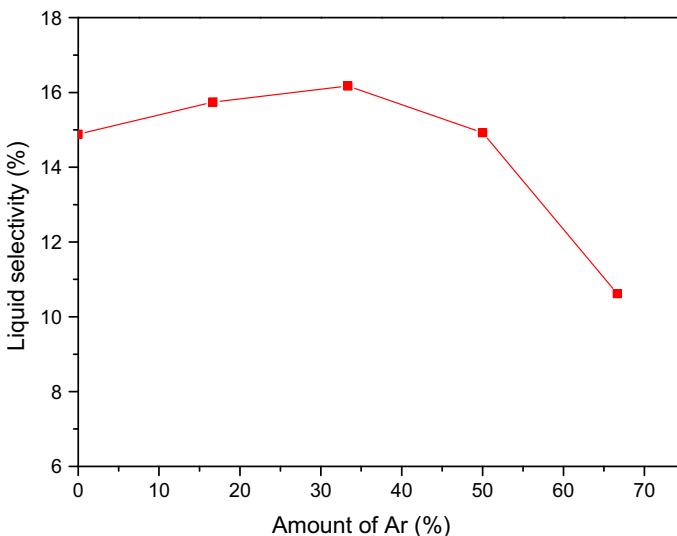


**Fig. 10** Evolution of liquid products selectivity as a function of the amount of Ar at applied power of 74 W

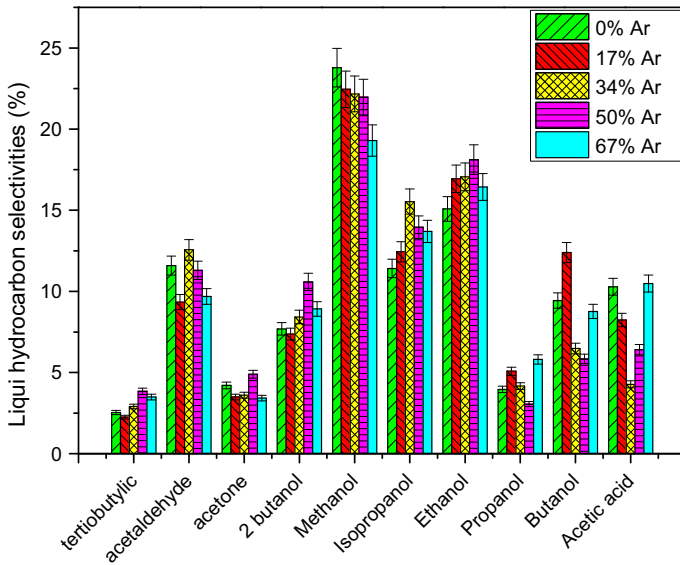


**Fig. 11** Evolution of liquid hydrocarbon selectivity as a function of the amount of Ar at applied power of 74 W

When Ar percentage increases from 0 to 66%, methanol selectivity decreases from 23 to 18%, while isopropanol increases from 14 to 16% then decreases slightly, and that of ethanol increases from 15 to 18% then decreases. These changes could be explained by the fact that an increase in argon content results in an increase in electron mean energy which results in a greater advancement of CH<sub>4</sub> degradation reaction and a diminution of liquid fuels concentration (Table 2). Another possible explanation is the dissociation of methanol, or other liquid products by collisions with energetic electrons. Zhang et al. [35] carried out dry reforming of methanol to produce syngas. They reported that there are seven initial

**Table 2** Intermediate dissociation reactions of CH<sub>4</sub> and the formation of methanol, ethanol and isopropanol and their activation threshold energies [31, 32]

Reaction	Number	Threshold activation energy (eV)
$e + CH_4 \rightarrow e + CH_3 + H$	(13)	8.8
$e + CH_4 \rightarrow e + CH_2 + H_2$	(14)	9.4
$e + CH_4 \rightarrow e + CH + H_2 + H$	(15)	12.5
$e + CH_4 \rightarrow e + C + 2H_2$	(9)	14
$CH_3 + OH + M \rightarrow CH_3OH + M$	(16)	–
$CH_3 + CH_2 \rightarrow C_2H_4 + H$	(17)	–
$C_2H_4 + H_2O \rightarrow C_2H_5OH$	(18)	–
$C_2H_6 + CH + M \rightarrow C_3H_7$	(19)	–
$C_3H_7 + H \rightarrow C_3H_6 + H_2$	(20)	–
$C_3H_6 + H_2O \rightarrow CH_3CH(OH)CH_3$	(21)	–
$H_2 + CO_2 \rightarrow CO + H_2O$	(22)	–

reaction paths for methanol dissociation by electronic collisions, which make this product fragile. The same thing can be said about the other products.

The increase of electron temperature from a certain threshold also leads to carbon deposition and to soot formation according to reaction (9), which reduces the selectivity of higher hydrocarbon products. Indeed, the increase of Ar content in the reactive volume causes radical reactants dilution, which makes more difficult interaction between them.

## Conclusion

In this study, we have presented experimental results of the influence of Ar on the properties of plasma as well as on the reactivity and the selectivity of gaseous and liquid products of methane reforming in the presence of carbon dioxide. Conversions of 47% for CH<sub>4</sub> and 28% for CO<sub>2</sub> were achieved. The main products are: CO, H<sub>2</sub>, C<sub>2</sub>H<sub>6</sub> and C<sub>2</sub>H<sub>4</sub>. More than 10 oxygenated liquid fuels were detected that represent 2–4% of the total mass of products.

Results showed that introducing Ar into the SDBD reduces the breakdown voltage, increases the density and electron temperature. That results in increasing the extent of reactions to enhance the CO, H<sub>2</sub> carbon and soot selectivity particularly when Ar percentage is greater than 33%. At the same time, using argon decreases the effective conversion of both reactants and the total quantity of higher fuels, i.e. C<sub>2</sub>H<sub>6</sub>, C<sub>2</sub>H<sub>4</sub> and liquid products. We observed that the total selectivity in liquid products reaches a maximum for Ar percentage of 33%, and decreases drastically for higher Ar percentage.

A mean electron energy of 1.3 eV and electron density of  $1.35 \times 10^{19} \text{ m}^{-3}$  were reached by adjusting Ar percentage at 33% with breakdown voltage smaller than 3.5 kV, that permitted to obtain the maximum liquid selectivity around 16 wt%, a carbon balance near 95% and a higher heating value energy efficiency of 6.05%. That seems to be the best compromise in our experimental conditions. The energy efficiency of the process is 7.85% without Ar on the reactive stream and decreases to reach 3.82% when Ar percentage is increased to 66% at applied power of  $74 \text{ W} \pm 2$ . The same trend has been observed at applied power of  $51 \text{ W} \pm 2$ . These results demonstrate that controlling the Ar percentage in reactant feed will permit to control the electrons energy and electron density at the lowest possible breakdown voltage in order to adapt them to the required chemical transformation.

During this work, we have demonstrated that it is possible to directly transform a CH<sub>4</sub>–CO<sub>2</sub> mixture into liquid oxygenated fuels, such as methanol and ethanol, in a SDBD reactor. Nevertheless, many investigations still need to be carried out, in particular to improve yields and reduce the energy cost of processing. The integration of suitable catalysts for the discharge reactors could help to achieve these objectives.

**Acknowledgements** This work was carried out with the financial support of Université Sorbonne Paris Cité in the framework of the Programme Interdisciplinaire: Les Energies de Demain.

## References

1. Connolly D, Lund H, Mathiesen BV (2016) Smart energy Europe: the technical and economic impact of one potential 100% renewable energy scenario for the European Union. *Renew Sustain Energy Rev* 60:1634–1653



2. EurObservER (2014) Biogas-barometer-2014. In: Barometer. EurObservER, p 6
3. Bradford M CJ, Vannice MA (1999) CO<sub>2</sub> reforming of CH<sub>4</sub>. *Catal Rev* 41(1):1–42
4. Hu YH, Ruckenstein E (2004) Catalytic conversion of methane to synthesis gas by partial oxidation and CO<sub>2</sub> reforming. *ChemInform* 48:297–345
5. Pettipas G et al (2007) A comparative study of non-thermal plasma assisted reforming technologies. *Int J Hydrog Energy* 32(14):2848–2867
6. Tao X, Bai M, Li X, Long H, Shang S, Yin Y, Dai X (2011) CH<sub>4</sub>–CO<sub>2</sub> reforming by plasma—challenges and opportunities. *Prog Energy Combust Sci* 37(2):113–124
7. Lebouvier A et al (2013) Assessment of carbon dioxide dissociation as a new route for syngas production: a comparative review and potential of plasma-based technologies. *Energy Fuels* 27(5):2712–2722
8. Snoeckx R, Bogaerts A (2017) Plasma technology—a novel solution for CO<sub>2</sub> conversion? *Chem Soc Rev* 46(19):5805–5863
9. Gibalov VI, Pietsch GJ (2012) Dynamics of dielectric barrier discharges in different arrangements. *Plasma Sources Sci Technol* 21(2):024010
10. Nikravech M, Rahmani A, Lazzaroni C, Baba K (2015) CH<sub>4</sub>–CO<sub>2</sub> reforming in surface-discharge reactor containing ZnO–Cu and NiO catalysts—influence of the applied power on products distribution. In: 22nd international symposium on plasma chemistry, P-II-8-32, p 5
11. Yap D, Tatibouët J-M, Batiot-Dupeyrat C (2018) Catalyst assisted by non-thermal plasma in dry reforming of methane at low temperature. *Catal Today* 299:263–271
12. Zeng YX et al (2018) Low temperature reforming of biogas over K-, Mg- and Ce-promoted Ni/Al<sub>2</sub>O<sub>3</sub> catalysts for the production of hydrogen rich syngas: understanding the plasma-catalytic synergy. *Appl Catal B* 224:469–478
13. Ray D, Reddy PMK, Challapalli S (2017) Glass beads packed DBD-plasma assisted dry reforming of methane. *Top Catal* 60(12–14):869–878
14. Allégraud K (2008) Décharge à barrière diélectrique de surface: physique et procédé. Ecole Polytechnique X
15. Malik MA, Malik SA, Jiang X (1999) Plasma reforming of natural gas to more valuable fuels. *J Nat Gas Chem* 8:166–178
16. Liu C-J, Xu G-H, Wang T (1999) Non-thermal plasma approaches in CO<sub>2</sub> utilization. *Fuel Process Technol* 58(2):119–134
17. Snoeckx R et al (2017) Plasma-based liquefaction of methane: the road from hydrogen production to direct methane liquefaction. *Plasma Process Polym* 14(6):1600115
18. Ramakers M, Michielsens I, Aerts R, Meynen V, Bogaerts A (2015) Effect of argon or helium on the CO<sub>2</sub> conversion in a dielectric barrier discharge. *Plasma Process Polym* 12(8):755–763
19. Jo S, Lee DH, Song Y-H (2015) Product analysis of methane activation using noble gases in a non-thermal plasma. *Chem Eng Sci* 130:101–108
20. Pinhão NR, Janeco A, Branco JB (2011) Influence of helium on the conversion of methane and carbon dioxide in a dielectric barrier discharge. *Plasma Chem Plasma Process* 31(3):427–439
21. Goujard V, Tatibouët J-M, Batiot-Dupeyrat C (2011) Carbon dioxide reforming of methane using a dielectric barrier discharge reactor: effect of helium dilution and kinetic model. *Plasma Chem Plasma Process* 31(2):315–325
22. Ozkan A et al (2015) CO<sub>2</sub>–CH<sub>4</sub> conversion and syngas formation at atmospheric pressure using a multi-electrode dielectric barrier discharge. *J CO<sub>2</sub> Util* 9:74–81
23. Zhang A-J et al (2010) Conversion of greenhouse gases into syngas via combined effects of discharge activation and catalysis. *Chem Eng J* 156(3):601–606
24. Janeco A, Pinhão NR, Guerra V (2014) Electron kinetics in He/CH<sub>4</sub>/CO<sub>2</sub> mixtures used for methane conversion. *J Phys Chem C* 119(1):109–120
25. Tu X, Whitehead JC (2012) Plasma-catalytic dry reforming of methane in an atmospheric dielectric barrier discharge: understanding the synergistic effect at low temperature. *Appl Catal B* 125:439–448
26. Snoeckx R et al (2015) Plasma-based dry reforming: improving the conversion and energy efficiency in a dielectric barrier discharge. *RSC Adv* 5(38):29799–29808
27. Sebastian AA, Wadehra JM (2005) Time-dependent behaviour of electron transport in methane–argon mixtures. *J Phys D Appl Phys* 38(10):1577–1587
28. Lowke J (1997) A unified theory of arcs and their electrodes. *Le Journal de Physique IV* 7(C4):C4-283–C4-294
29. Kim JH, Choi YH, Hwang YS (2006) Electron density and temperature measurement method by using emission spectroscopy in atmospheric pressure nonequilibrium nitrogen plasmas. *Phys Plasmas* 13(9):093501

30. Hagelaar G, Pitchford L (2005) Solving the Boltzmann equation to obtain electron transport coefficients and rate coefficients for fluid models. *Plasma Sources Sci Technol* 14(4):722–733
31. Snoeckx R et al (2013) Plasma-based dry reforming: a computational study ranging from the nanoseconds to seconds time scale. *J Phys Chem C* 117(10):4957–4970
32. Janev RK, Reiter D (2002) Collision processes of CHy and CHy+ hydrocarbons with plasma electrons and protons. *Phys Plasmas* 9(9):4071–4081
33. Anicich VG (2003) An index of the literature for bimolecular gas phase cation-molecule reaction kinetics. JPL Publication 03-19, JPL, NASA, Pasadena
34. Tsang W, Hampson R (1986) Chemical kinetic data base for combustion chemistry. Part I. Methane and related compounds. *J Phys Chem Ref Data* 15(3):1087–1279
35. Zhang H, Li X, Zhu F, Cen K, Du C, Tu X (2017) Plasma assisted dry reforming of methanol for clean syngas production and high-efficiency CO<sub>2</sub> conversion. *Chem Eng J* 310:114–119